OPEN ACCESS
Fractals, Vol. 29, No. 5 (2021) 2140022 (16 pages)

DOI: 10.1142/S0218348X21400223

World Scientific
www.worldscientific.com

DESIGN OF NEURO-SWARMING HEURISTIC SOLVER FOR MULTI-PANTOGRAPH SINGULAR DELAY DIFFERENTIAL EQUATION

ZULQURNAIN SABIR[*,††], DUMITRU BALEANU[†,‡,§,‡‡], MUHAMMAD ASIF ZAHOOR RAJA[¶,‖,§§], JUAN L. G. GUIRAO[**,¶¶]

[*]*Department of Mathematics and Statistics*
Hazara University, Mansehra, Pakistan

[†]*Department of Mathematics, Cankaya University*
Ankara, Turkey

[‡]*Institute of Space Science, Magurele-Bucharest, Romania*

[§]*Department of Medical Research, China Medical University Hospital*
China Medical University, Taichung, Taiwan

[¶]*Future Technology Research Center*
National Yunlin University of Science and Technology
123 University Road, Section 3, Douliou, Yunlin 64002, Taiwan, R.O.C.

[‖]*Department of Electrical and Computer Engineering*
COMSATS University Islamabad, Attock Campus, Attock 43600, Pakistan

[**]*Department of Applied Mathematics and Statistics*
Technical University of Cartagena
Hospital de Marina 30203-Cartagena, Spain

[††]*zulqurnain_maths@hu.edu.pk*
[‡‡]*dumitru@cankaya.edu.tr*
[§§]*rajamaz@yuntech.edu.tw*
[¶¶]*juan.garcia@upct.es*

[‡‡]Corresponding author.

Received September 11, 2020
Accepted December 17, 2020
Published March 16, 2021

Abstract

This research work is to design a neural-swarming heuristic procedure for numerical investigations of Singular Multi-Pantograph Delay Differential (SMP-DD) equation by applying the function approximation aptitude of Artificial Neural Networks (ANNs) optimized efficient swarming mechanism based on Particle Swarm Optimization (PSO) integrated with convex optimization with Active Set (AS) algorithm for rapid refinements, named as ANN-PSO-AS. A merit function (MF) on mean squared error sense is designed by using the differential ANN models and boundary condition. The optimization of this MF is executed with the global PSO and local search AS approaches. The planned ANN-PSO-AS approach is instigated for three different SMP-DD model-based equations. The assessment with available standard results relieved the effectiveness, robustness and precision that is further authenticated through statistical investigations of Variance Account For, Root Mean Squared Error, Semi-Interquartile Range and Theil's inequality coefficient performances.

Keywords: Multi-pantograph Systems; Particle Swarm Optimization; Neural Networks; Active-set Algorithm; Numerical Computing; Statistical Measures.

1. INTRODUCTION

The singular multi-pantograph delay differential (SMP-DD) equation is considered very important due to its wide-ranging applications in the theory of statistics, physics, electrodynamics, astrophysics, number theory, direction-finding control of ships, engineering, quantum mechanics, finances, chemical sciences, nonlinear dynamical models, chemical kinetics, cell growth, electronic models, infectious viruses and medicine.[1–7] The literature form of the second kind of SMP-DD equation is given as[8]

$$\begin{aligned} &Y''(\chi) + \sum_{k=1}^{n} \frac{1}{P_k(\chi)} Y'(r_k\chi) + \frac{1}{Q(\chi)} Y(\chi) = G(\chi), \\ &0 < \chi, \quad r_k < 1, \quad k = 1, 2, 3, \ldots, n, \\ &Y(0) = A_1, \quad Y'(0) = A_2, \end{aligned} \tag{1}$$

where $P_k(\chi)$ and $Q(\chi)$ are the continuous functions and only a few schemes based on analytical or numerical exist in the literature to solve SMP-DD equation. Some reported studies in this regard for SMP-DD equation can be seen in Refs. 9–11. It is not easy to solve the SMP-DD equation-based model (1) due to its harder nature, i.e. multi-pantographs and multi-singular points. All the cited approaches in Refs. 9–11 have their specific efficiency, accuracy, performance and limitations. Alongside these mentioned stochastic approaches, the numerical solvers using the heuristic/swarm schemes[12–14] look proficient to integrate the area of multi-pantographs and multi-singular points-based nonlinear systems. Some up-to-dated applications of these solvers are nonlinear optics,[15] Thomas–Fermi singular model,[16] financial market prediction,[17] mosquito dispersal model,[18] singular three-point model,[19] nonlinear system of prey–predator equations,[20] singular fourth-order model,[21] plasma physics problems,[22] magnetohydrodynamic studies,[23] singular model of Lane–Emden using the Morlet wavelet function,[24] fluid dynamics,[25] model of heartbeat dynamics,[26] corneal shape model,[27] multi-singularity-based nonlinear models,[28] nonlinear models arising in electric circuits,[29] nonlinear reactive transport model,[30] SIR nonlinear mathematical model for the dynamics of the dengue fever,[31] HIV infection model of CD4+ T cells,[32] functional differential-based singular system[33,34] and nonlinear Riccati equation,[35] doubly singular multi-fractional order Lane–Emden system,[36] nonlinear unipolar electrohydrodynamic pump flow model,[37] future generation disease control mechanism for nonlinear system of COVID-19 epidemic model,[38] 3D flow of

Eyring–Powell magneto-nanofluidic model[39] and nonlinear dusty plasma system.[40] The aim of this research is to discuss the second-order SMP-DD system together with the numerical simulations for superior model understanding using the stochastic approach through Artificial Neural Networks (ANNs) trained with Particle Swarm Optimization (PSO) aided with the Active-Set (AS) algorithm, called as ANN-PSO-AS scheme. Few potential structures of the suggested ANN-PSO-AS algorithm are briefly narrated as follows:

- A novel integrated intelligent approach ANN-PSO-AS is proposed for the numerical treatment of the second-order SMP-DD equation-based models.
- Overlapping outcomes using the proposed scheme ANN-PSO-AS from reference results for different SMP-DD-based examples demonstrated the worth by means of accuracy and convergence indicators.
- Performance of the ANN-PSO-AS solver is endorsed via statistical investigation on multiple executions means of Variance Account For (VAF), Root Mean Squared Error (RMSE), Semi-Interquartile Range (SI-R) and Theil's inequality coefficient (TIC) performance metrics.
- Beside the accurate outcomes for the second-order SMP-DD equation, ease of understanding the concepts, consistency, smooth operation, exhaustive applicability and robustness are other appreciated perks.

The rest of the work is organized as follows: Sec. 2 presents the ANN-PSO-AS algorithm; performance indices are provided in Sec. 3. The numerical solutions of the second-order SMP-DD model is given in Sec. 4. Whereas, conclusions and future research plans are given in Sec. 5.

2. SOLUTION PROCEDURE

The framework for solving the second-order SMP-DD model is provided in two sections.

- Introducing a mean squared error sense merit/cost function (MF) for solving the differential equation with initial conditions.
- The combination of ANN-PSO-AS algorithm is accessible to optimize the MF for second-order SMP-DD model.

2.1. ANN Modeling Procedures

The ANNs type of models presented by many researchers to solve the linear/nonlinear structures in various areas.[41,42] The feed-forward ANN based models are used to approximate the continuous mapping solutions and the corresponding derivatives taking the log-sigmoid activation function $S(\chi) = (1 + e^{-\chi})^{-1}$ are shown as

$$\begin{aligned}
\hat{Y}(\chi) &= \sum_{i=1}^{k} z_i S(w_i\chi + a_i) \\
&= \sum_{i=1}^{k} z_i (1 + e^{-(w_i\chi + a_i)})^{-1}, \\
\hat{Y}'(\chi) &= \sum_{i=1}^{k} z_i S'(w_i\chi + a_i) \\
&= \sum_{i=1}^{k} z_i w_i e^{-(w_i\chi + a_i)} \\
&\quad \times (1 + e^{-(w_i\chi + a_i)})^{-2}, \\
\hat{Y}''(\chi) &= \sum_{i=1}^{k} z_i S''(w_i\chi + a_i) \\
&= \sum_{i=1}^{k} z_i w_i^2 \begin{pmatrix} 2e^{-2(w_i\chi + a_i)} \\ \quad \times (1 + e^{-(w_i\chi + a_i)})^{-3} \\ - e^{-(w_i\chi + a_i)} \\ \quad \times (1 + e^{-(w_i\chi + a_i)})^{-2} \end{pmatrix},
\end{aligned} \tag{2}$$

where the weights are $\boldsymbol{z} = [z_1, z_2, z_3, \ldots, z_m]$, $\boldsymbol{w} = [w_1, w_2, w_3, \ldots, w_m]$ and $\boldsymbol{a} = [a_1, a_2, a_3, \ldots, a_m]$. For solving the second-order SMP-DD model presented in Eq. (1), an error-based function is introduced as follows:

$$e_{\mathrm{FIT}} = e_{\mathrm{FIT}-1} + e_{\mathrm{FIT}-2}, \tag{3}$$

where $e_{\mathrm{FIT}-1}$ and $e_{\mathrm{FIT}-2}$ are an unsupervised error functions related to second-order SMP-DD model and initial conditions, given as

$$\begin{aligned}
e_{\mathrm{FIT}-1} = \frac{1}{N}\sum_{i=1}^{N} \Bigg(\hat{Y}_i'' + \sum_{k=1}^{n} \frac{1}{P_{k,i}} \hat{Y}'_{k,i} \\
+ \frac{1}{Q_i}\hat{Y}_i - G_i \Bigg)^2, \quad r_k < 1, \\
k = 1, 2, \ldots, n, i = 1, 2, \ldots, N,
\end{aligned} \tag{4}$$

where $Nh = 1, P_{k,i} = P_i(\chi_k), Q_i = Q(\chi_i), \hat{Y}_i = \hat{Y}(\chi_i), \hat{Y}_{k,i} = \hat{Y}(r_k\chi_i), \chi_i = kh$. Similarly, $e_{\mathrm{FIT}-2}$ is

the error function associated to the initial conditions, written as

$$e_{\mathrm{FIT}-2} = \frac{1}{2}((\hat{Y}_0)^2 + (\hat{Y}_N)^2). \tag{5}$$

2.2. Network Optimization: PSO-AS Approach

The combined framework of PSO and AS approach ratifies the optimization of the parameters for solving the second-order SMP-DD model given in Eq. (1).

There are many global search schemes, among them PSO is a well-known global search algorithm used as an optimization solver. PSO works as an alteration of genetic algorithm process, which is introduced by Eberhart and Kennedy in the previous century.[43,44] It is metaheuristic in nature due to its optimization capabilities in large search spaces. The execution process of the PSO as compared to GA is relatively efficient to implement due to the less memory requirement. In the optimization of PSO approach, initial swarm spreads in the larger domain. To improve the PSO, the procedure gives iteratively optimal results $\boldsymbol{P}_{\mathrm{LB}}^{\phi-1}$ and $\boldsymbol{P}_{\mathrm{GB}}^{\phi-1}$, which designate the position and velocity of the swarm, written as

$$\boldsymbol{X}_i^{\phi} = \boldsymbol{X}_i^{\phi-1} + \boldsymbol{V}_i^{\phi-1}, \tag{6}$$

$$\boldsymbol{V}_i^{\phi} = \Psi \boldsymbol{V}_i^{\phi-1} + \phi_1(\boldsymbol{P}_{LB}^{\phi-1} - \boldsymbol{X}_i^{\phi-1})\boldsymbol{r}_1 + \phi_2(\boldsymbol{P}_{\mathrm{GB}}^{\phi-1} - \boldsymbol{X}_i^{\phi-1})\boldsymbol{r}_2, \tag{7}$$

where Ψ is the inertia weight vector, $\boldsymbol{X}_i$ is the position and $\boldsymbol{V}_{\boldsymbol{i}}$. represents velocity. Whereas, ϕ_1 and ϕ_2 are the constant for acceleration factors. PSO has widespread applications in parameter estimation of plane waves,[45] nonlinear electric circuits,[46] nonlinear optimization problems,[47] reactive power dispatch problems,[48] active-noise control systems,[49] optimization in atomic power plants[50] and design of novel epidemic models.[51]

The convergence performance of the PSO scheme is boosted by the hybridization of a local search technique. In this regard, "AS" algorithm is used for quick modification of the results. AS is a valuable scheme that confines the system model for better understanding along with optimization of the proposed system. Recently, AS method is applied for convex unconstrained and constrained optimization problems reported in Refs. 52–55.

Table 1 Optimization Process Using the Designed ANN-PSO-AS Approach.

```
Start of PSO
    Step 1: Initialization: Randomly generate the primary swarms. Transform the parameters of the
'PSO' and 'optimoptions'.
    Step 2: Fitness formulation: Using equation (3), scrutinize the ''fitness values'' of each
particle.
    Step 3: Ranking: Rank individually the particle for minimum values of the ''Merit function''.
    Step 4: Stopping Standards: Dismiss if

        • ''Fitness level'' accomplished.
        • Selected ''flights/cycles'' executed.

        When ''stopping'' standard meets, move to Step 5
    Step 5: Renewal: By using equations (6) and (7), call the ''position'' and ''velocity''
    Step 6: Improvement: Repeat the step (2) → (6), until the whole 'flights' are achieved.
    Step 7: Storage: Save the best ''Merit function values'', represented as ''best global particle''
PSO process Ends
Start the PSO-AS approach
    Inputs: Global best values
    Output: W_PSO−AS signifies the best PSO-AS approach values
    Initialize: Used ''Global best values'' as a start point
    Termination: Stop if {Fitness = e_FIT = 10^−18}, {Generation = 700},
{TolCon = TolX = TolFun = 10^−21} and {MaxFunEvals = 275000} gets the above standards.
    While {Stop}
    Calculation of Fitness: Use e_FIT for the ''fitness values'' given in equation (3)
    Adjustments: Invoke the 'fmincon' routine for the AS approach to finetune the values of the
''weight vector''.
Move to ''fitness step'' using the ''weight vector's'' updated form.
    Store: Store the W_PSO−AS, iterations, e_FIT, function count and time for the present trial.
PSO-AS approach Ends
```

In this work, the PSO-AS method is a functional to present the solution of the second-order SMP-DD model provided in Eq. (1). The details of the pseudocode using the ANN-PSO-AS method are tabulated in Table 1.

3. PERFORMANCE METRICS

This section presents the mathematical form of the statistical operators based on VAF, RMSE and TIC for solving three variants of second-order SMP-DD system. The mathematical forms are introduced as

$$\begin{cases} \text{VAF} = \left(1 - \dfrac{\text{var}(Y_i(\chi) - \hat{Y}_i(\chi))}{\text{var}(Y_i(\chi))}\right) * 100, \\ \text{EVAF} = |\text{VAF} - 100|, \end{cases} \tag{8}$$

$$\text{RMSE} = \sqrt{\frac{1}{n}\sum_{i=1}^{n}(Y_i - \hat{Y}_i)^2} \tag{9}$$

$$\text{TIC} = \frac{\sqrt{\frac{1}{n}\sum_{i=1}^{n}(Y_i - \hat{Y}_i)^2}}{\left(\sqrt{\dfrac{1}{n}\sum_{i=1}^{n}Y_i^2} + \sqrt{\frac{1}{n}\sum_{i=1}^{n}\hat{Y}_i^2}\right)}, \tag{10}$$

4. RESULTS AND DISCUSSIONS

The detailed discussion of the results to solve three different examples based on second-order SMP-DD model is provided in this section.

Example 1. Consider the second-order SMP-DD equation involving exponential functions which is written as:

$$\begin{aligned} &Y''(\chi) + \tfrac{1}{\chi}Y'\left(\frac{\chi}{2}\right) + \tfrac{1}{\chi^2}Y' \\ &\quad \times \left(\frac{\chi}{4}\right) + \tfrac{1}{1-\chi}Y(\chi) = H(\chi), \\ &\quad 0 < \chi \le 1, \\ &Y(0) = 1, \quad Y'(0) = 1, \end{aligned} \tag{11}$$

where

$$H(\chi) = -\frac{(e^{\frac{\chi}{4}}(\chi-1))}{4} - \frac{(\chi e^{\frac{\chi}{2}}(\chi-1))}{2} - e^{\chi}(\chi-2)\chi^2.$$

The exact solution of the second-order SMP-DD equation (11) is e^{χ} and the MF function becomes

$$\begin{aligned} e_{\text{FIT}} = \frac{1}{N}\sum_{m=1}^{N} &\begin{pmatrix} \chi_m^2(1-\chi_m)\hat{Y}''(\chi_m) \\ \quad + \chi_m(1-\chi_m)\hat{Y}'\left(\frac{1}{2}\chi_m\right) \\ \quad + (1-\chi_m)\hat{Y}'\left(\frac{1}{4}\chi_m\right) \\ \chi_m^2 F_m - \chi_m^2(1-\chi_m)H_m \end{pmatrix}^2 \\ &+ \frac{1}{2}((\hat{Y}_0 - 1)^2 + (\hat{Y}_0' - 1)^2). \end{aligned} \tag{12}$$

Example 2. Let a second-order SMP-DD system with trigonometric expressions be

$$\begin{aligned} &Y''(\chi) + \frac{1}{\chi}Y'\left(\frac{\chi}{2}\right) + \frac{1}{\chi^2}Y' \\ &\quad \times \left(\frac{\chi}{4}\right) + \frac{1}{1-\chi}Y(\chi) = R(\chi), \\ &\quad 0 < \chi \le 1, \quad Y(0) = 1, \quad Y'(0) = 0, \end{aligned} \tag{13}$$

where

$$\begin{aligned} R(\chi) = &\frac{\chi}{1-\chi}\cos\chi - \frac{1}{\chi}\sin\left(\frac{\chi}{2}\right) \\ &- \frac{1}{\chi^2}\sin\left(\frac{\chi}{4}\right). \end{aligned}$$

The exact solution of the second-order SMP-DD equation (13) is $\text{Cos}(\chi)$ and the MF function becomes

$$\begin{aligned} e_{\text{FIT}} = \frac{1}{N}\sum_{m=1}^{N} &\begin{pmatrix} \chi_m^2(1-\chi_m)\hat{Y}''(\chi_m) \\ \quad + \chi_m(1-\chi_m)\hat{Y}'\left(\frac{1}{2}\chi_m\right) \\ \quad + (1-\chi_m)\hat{Y}'\left(\frac{1}{4}\chi_m\right) \\ \quad + \chi_m^2 F_m - \chi_m^2(1-\chi_m)R_m \end{pmatrix}^2 \\ &+ \frac{1}{2}((\hat{Y}_0 - 1)^2 + (\hat{Y}_0')^2). \end{aligned} \tag{14}$$

Example 3. Let a second-order SMP-DD system with hyperbolic trigonometric expressions be

$$\begin{aligned} &Y''(\chi) + \frac{1}{\chi}Y'\left(\frac{\chi}{2}\right) + \frac{1}{\chi^2}Y'\left(\frac{\chi}{4}\right) \\ &\quad + \frac{1}{1-\chi}Y(\chi) = G(\chi), \quad 0 < \chi \le 1, \\ &\quad Y(0) = 0, \quad Y'(0) = 1, \end{aligned} \tag{15}$$

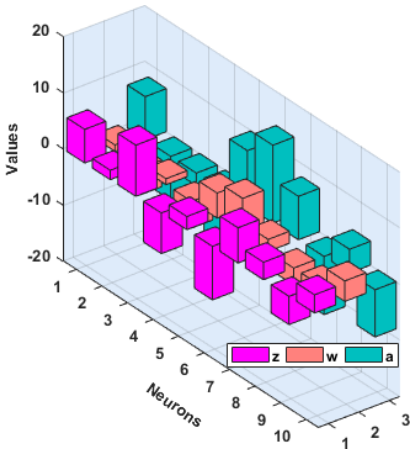

(a) Example 1: Best weights

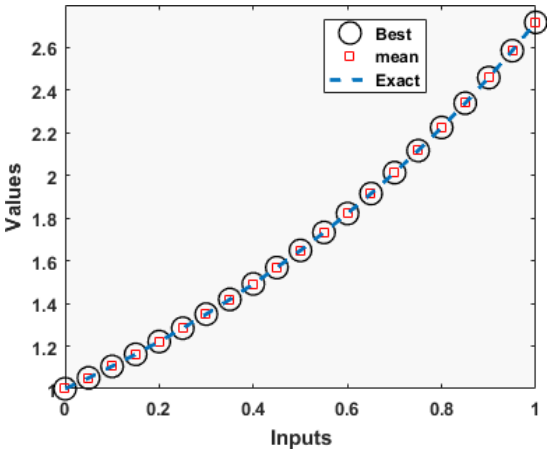

(d) Example 1: Result comparison

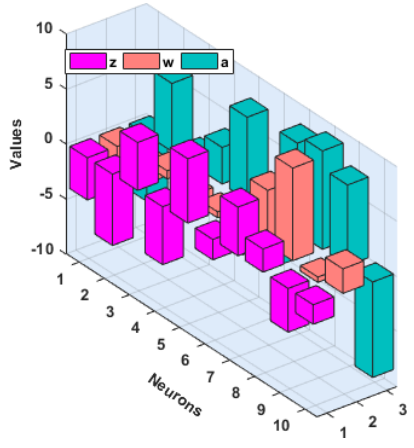

(b) Example 2: Best weights

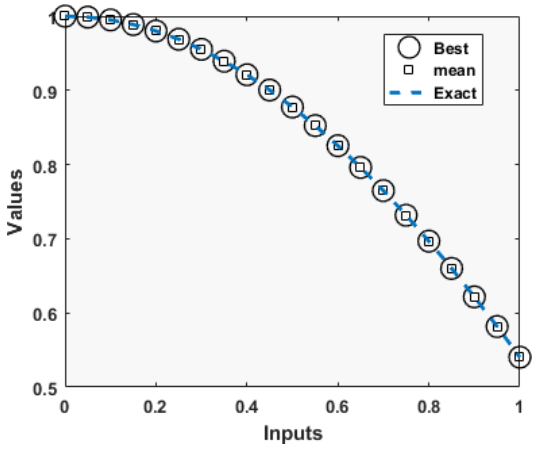

(e) Example 2: Result comparison

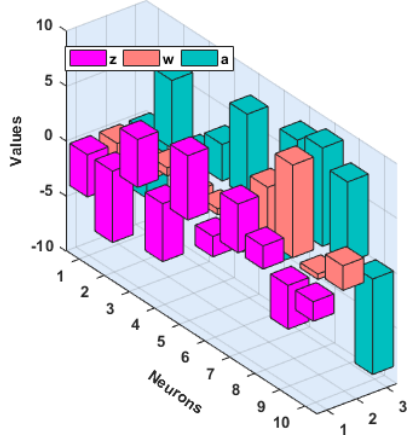

(c) Example 3: Best weights

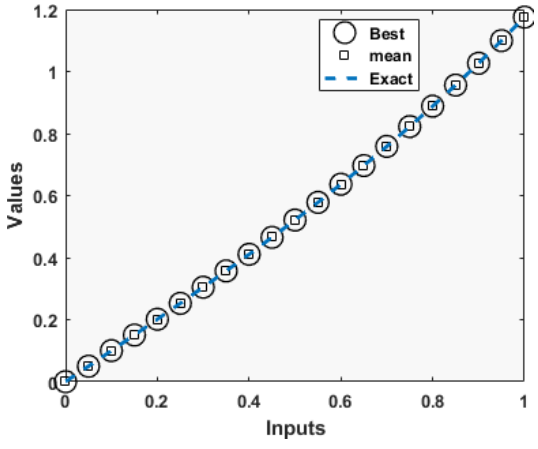

(f) Example 3: Result comparison

Fig. 1 A best weights set along with the exact, mean and proposed solutions of the second-order SMP-DD model-based examples (Examples 1–3).

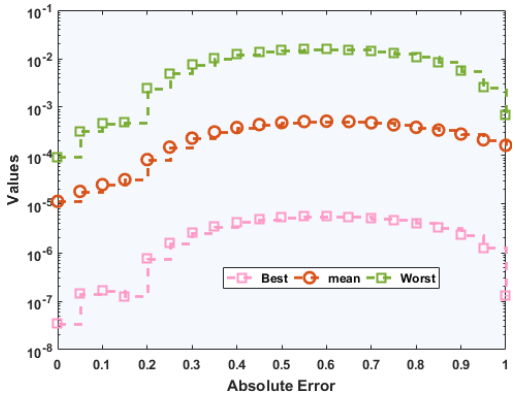

(a) AE for SMP-DD Example 1

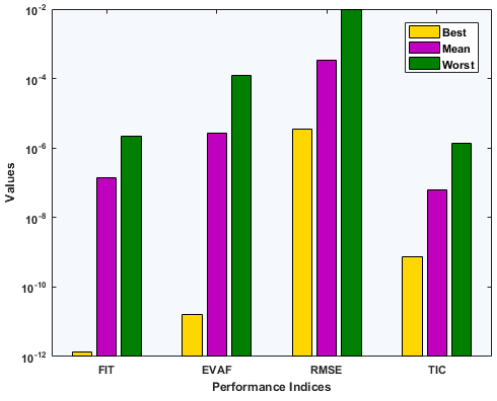

(d) Performance analysis for SMP-DD Example 1

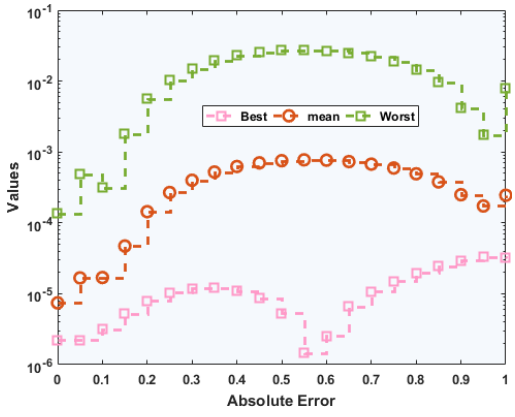

(b) AE for SMP-DD Example 2

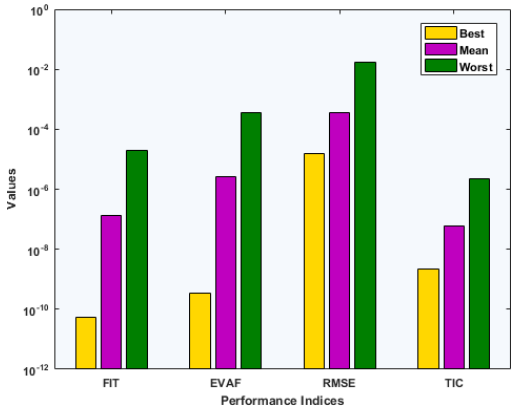

(e) Performance analysis for SMP-DD Example 2

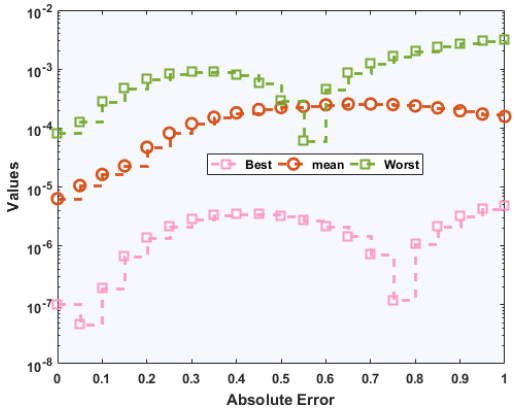

(c) AE for SMP-DD Example 3

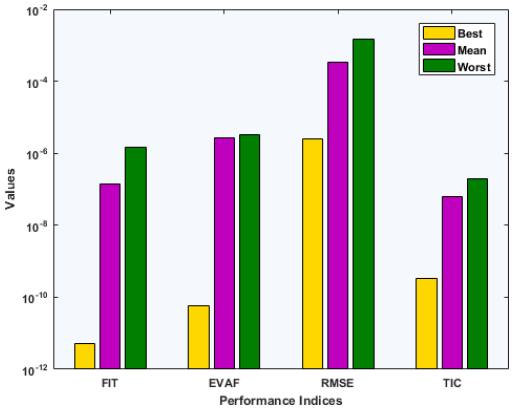

(f) Performance analysis for SMP-DD Example 3

Fig. 2 The AE along with other performance metrics of ANN-PSO-AS approach for second-order SMP-DD model-based examples (Examples 1–3).

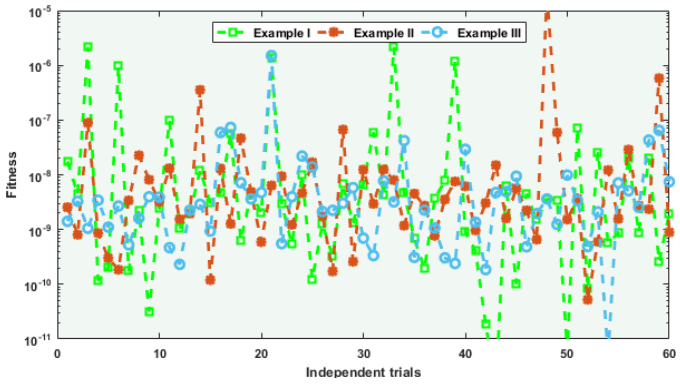

(a) Fitness values in convergence measures for Examples 1–3

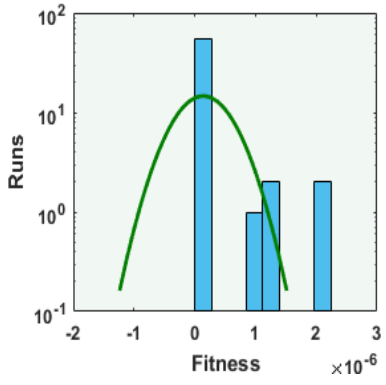

(b) Example 1: Histograms

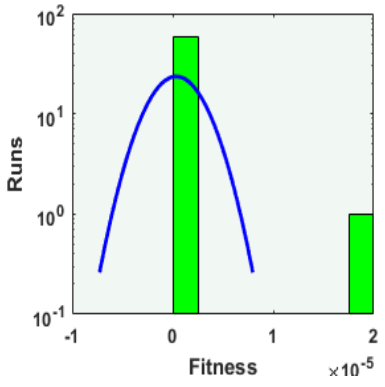

(c) Example 2: Histograms

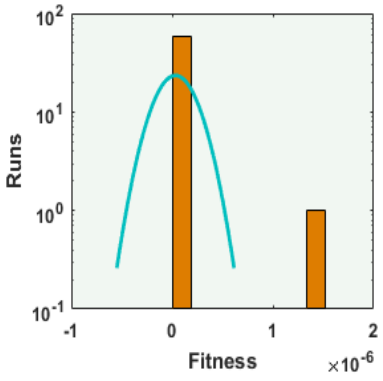

(d) Example 3: Histograms

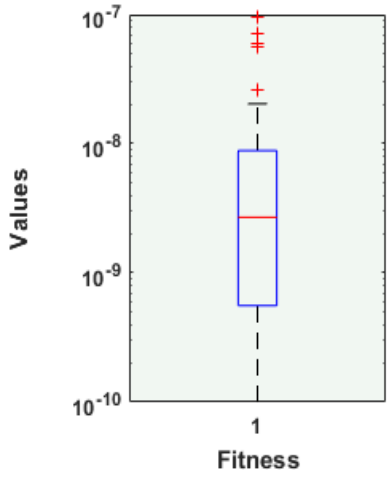

(e) Example 1: Boxplots

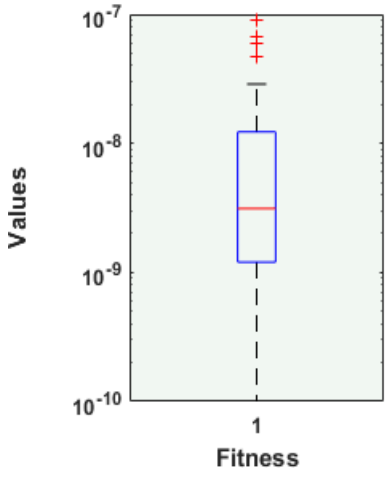

(f) Example 2: Boxplots

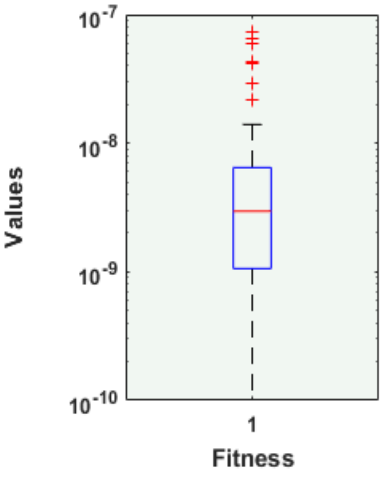

(g) Example 3: Boxplots

Fig. 3 Statistical assessments on ANN-PSO-AS approach via fitness together with the boxplots/histograms for SMP-DD model-based examples (Examples 1–3).

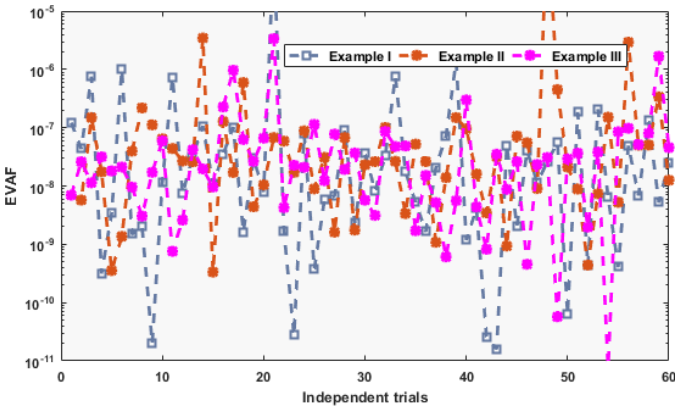

(a) EVAF values in convergence measures for Examples 1–3

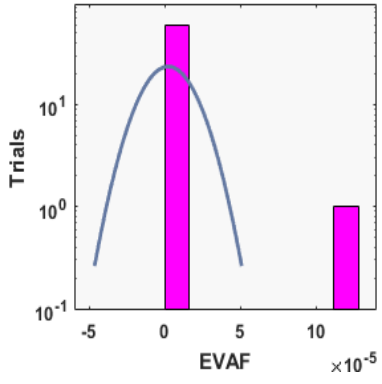

(b) Example 1: Histograms

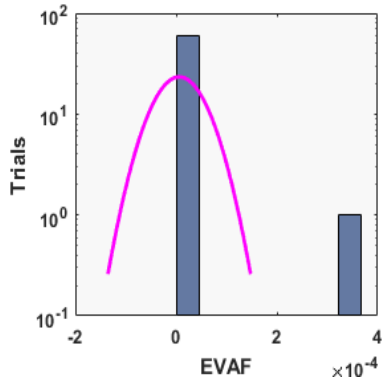

(c) Example 2: Histograms

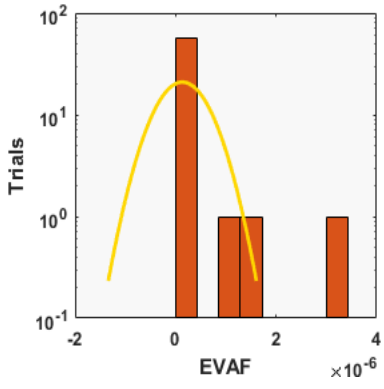

(d) Example 3: Histograms

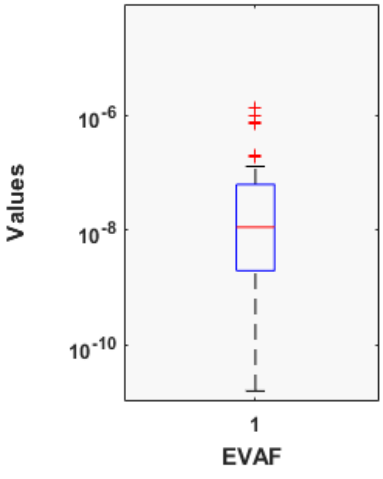

(e) Example 1: Boxplots

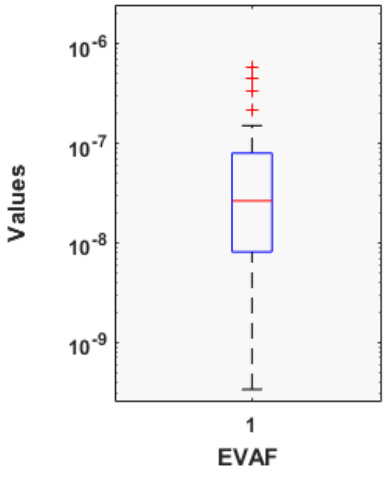

(f) Example 2: Boxplots

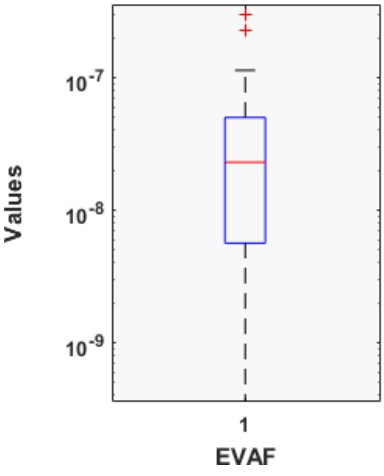

(g) Example 3: Boxplots

Fig. 4 Statistical assessments on ANN-PSO-AS approach via EVAF together with the boxplots/histograms for SMP-DD model-based examples (Examples 1–3).

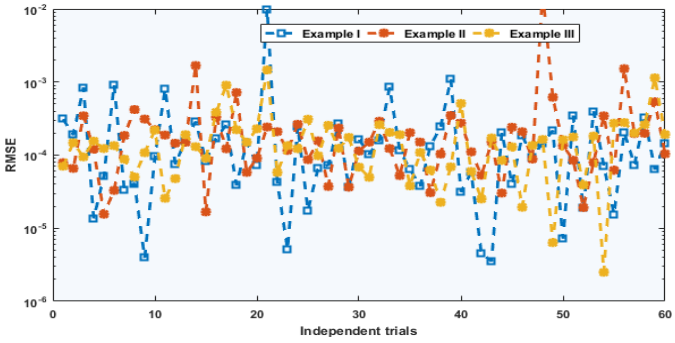

(a) RMSE values in convergence measures for Examples 1–3

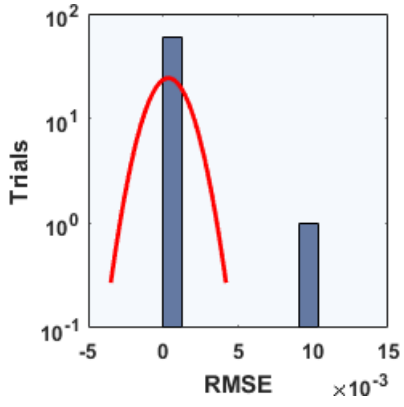

(b) Example 1: Histograms

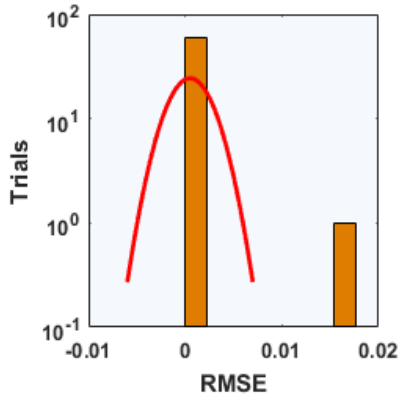

(c) Example 2: Histograms

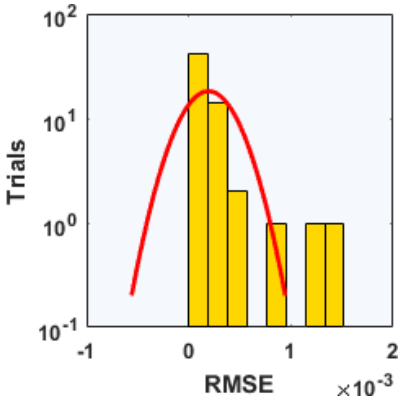

(d) Example 3: Histograms

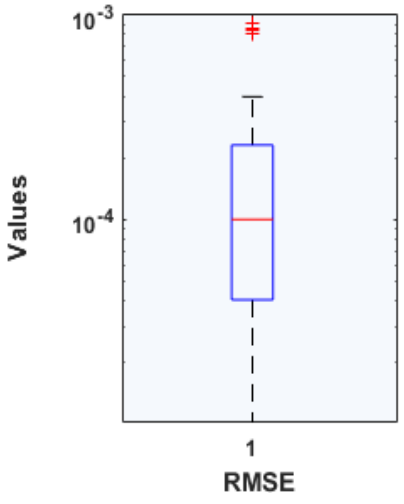

(e) Example 1: Boxplots

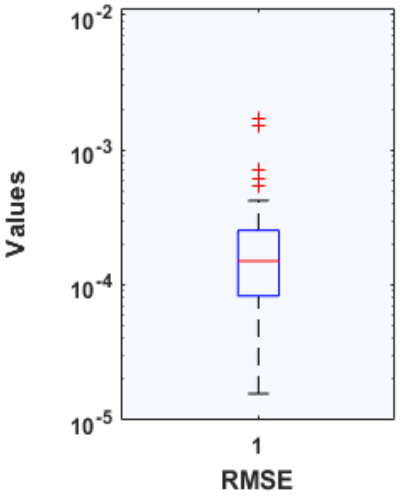

(f) Example 2: Boxplots

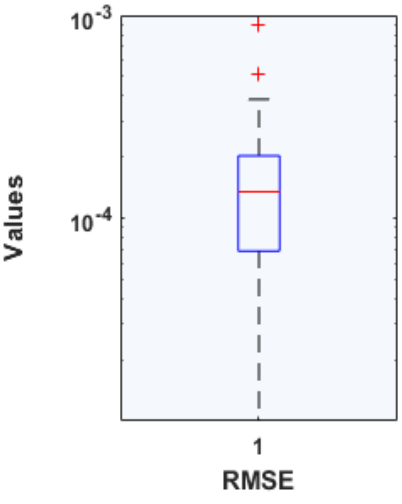

(g) Example 3: Boxplots

Fig. 5 Statistical assessments on ANN-PSO-AS approach via RMSE together with the boxplots/histograms for SMP-DD model-based examples (Examples 1–3).

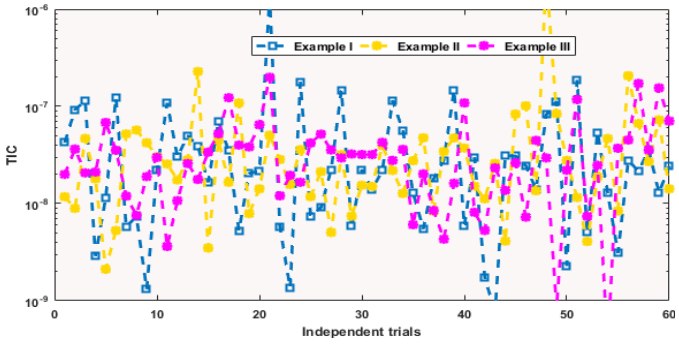

(a) TIC values in convergence measures for Examples 1–3

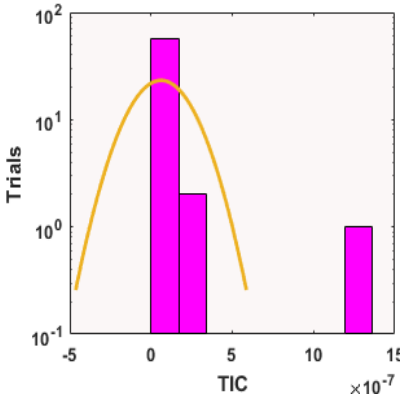

(b) Example 1: Histograms

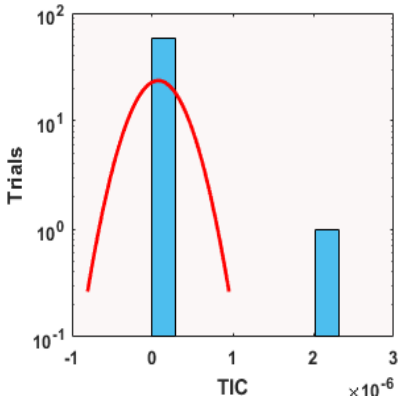

(c) Example 2: Histograms

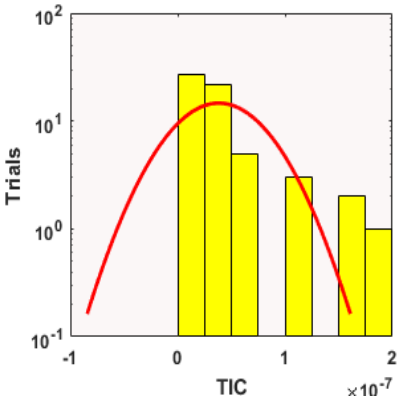

(d) Example 3: Histograms

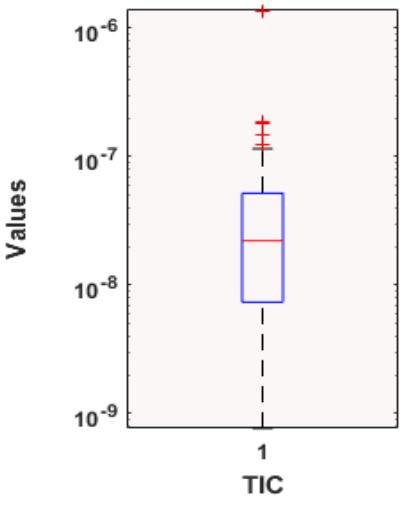

(e) Example 1: Boxplots

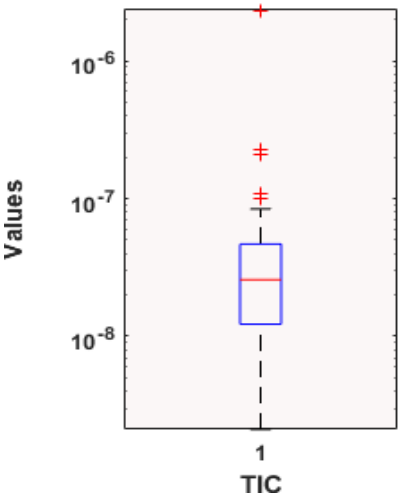

(f) Example 2: Boxplots

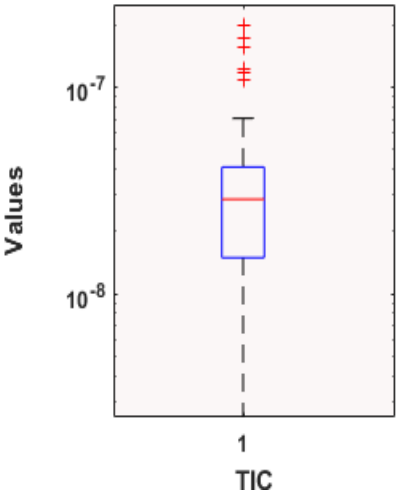

(g) Example 3: Boxplots

Fig. 6 Statistical assessments on ANN-PSO-AS approach via TIC together with the boxplots/histograms for SMP-DD model-based examples (Examples 1–3).

where

$$G(\chi) = \frac{2-\chi}{1-\chi}\text{Sinh}(\chi) + \frac{1}{\chi}\text{Cosh}\left(\frac{\chi}{2}\right) + \frac{1}{\chi^2}\text{Cosh}\left(\frac{\chi}{4}\right).$$

The exact solution of the second-order SMP-DD equation (15) is $\sinh(\chi)$ and the MF function becomes

$$e_{\text{FIT}} = \frac{1}{N}\sum_{m=1}^{N}\begin{pmatrix}\chi_m^2(1-\chi_m)\hat{Y}''(\chi_m) \\ +\chi_m(1-\chi_m)\hat{Y}'\left(\frac{1}{2}\chi_m\right) \\ +(1-\chi_m)\hat{Y}'\left(\frac{1}{4}\chi_m\right) \\ +\chi_m^2 F_m - \chi_m^2(1-\chi_m)G_m\end{pmatrix}^2 + \frac{1}{2}((\hat{Y}_0)^2 + (\hat{Y}_0' - 1)^2). \quad (16)$$

The designed ANN-PSO-AS approach is applied for 60 runs to get the system parameters using the ANN-PSO-AS to solve the second-order SMP-DD model-based examples (Examples 1–3). The set of trained decision variables is used to demonstrate the estimated numerical solution of the model (1). The mathematical formulation of the projected solutions is written as

$$\hat{Y}_1(\chi) = \frac{5.9788}{1+e^{-(1.143\chi+7.658)}} + \frac{1.6700}{1+e^{-(-4.767\chi-7.766)}} + \frac{9.0929}{1+e^{-(1.064\chi-2.228)}} + \cdots + \frac{3.2410}{1+e^{-(3.636\chi-8.395)}}, \quad (17)$$

$$\hat{Y}_2(\chi) = \frac{0.2002}{1+e^{-(4.177\chi+0.622)}} + \frac{11.7221}{1+e^{-(4.137\chi-12.892)}} + \frac{-6.536}{1+e^{-(11.822\chi+11.817)}} + \cdots - \frac{0.9502}{1+e^{-(-11.802\chi-9.837)}}, \quad (18)$$

$$\hat{Y}_3(\chi) = \frac{-3.8295}{1+e^{-(-2.323\chi-6.028)}} - \frac{6.4774}{1+e^{-(-2.045\chi+6.163)}} + \frac{4.3507}{1+e^{-(0.7494\chi+1.013)}} + \cdots - \frac{1.7718}{1+e^{-(2.227\chi-8.666)}}. \quad (19)$$

Optimization is performed to solve the second-order SMP-DD model-based problems (Examples 1–3) for the interval [0, 1] with 0.05 step size applying the PSO-AS hybridization for 60 independent executions. A best weights set and the exact, mean and proposed results comparison for the second-order SMP-DD model-based examples (Examples 1–3) are provided in Fig. 1. It is observed that for all the examples, all the said solutions overlapped with each other. This coinciding of the outcomes indicates the perfection of the ANN-PSO-AS approach. The values of the absolute error (AE) and performance investigations through ANN-PSO-AS approach for second-order SMP-DD model-based examples (Examples 1–3) are plotted in Fig. 2. The values of the AE are plotted in Figs. 2(a)–2(c), while the performance measures are drawn in Figs. 2(d)–2(f).

It is seen that the best values for Examples 1–3 are found near to 10^{-6}–10^{-7}, 10^{-5}–10^{-6} and 10^{-6}–10^{-7}, while the mean and worst for all the examples are found around 10^{-4}–10^{-5} and 10^{-2}–10^{-4}, respectively. The best fitness and EVAF for all the examples observed near to 10^{-9}–10^{-12}, while for all examples, the best RMSE and TIC lie around 10^{-4}–10^{-6} and 10^{-8}–10^{-10}, respectively. The mean Fitness and TIC values for all the examples are about 10^{-6}–10^{-8}, while the mean for EVAF and RMSE lie around 10^{-4}–10^{-6} and 10^{-2}–10^{-4}, respectively. Moreover, even the worst indices for all the gages are also found to be satisfactory.

The statistical investigation for ANN-PSO-AS approach via Fitness, EVAF, RMSE and TIC operators together with the boxplots/histogram values for SMP-DD model-based examples (Examples 1–3) are provided in Figs. 3–6. These statistical studies are accomplished for 60 independent executions using 10 numbers of neurons. It is seen that the Fitness, EVAF, RMSE and TIC values lie around 10^{-06} –10^{-10}, 10^{-07}–10^{-09}, 10^{-03}–10^{-05} and 10^{-07}–10^{-09}, respectively.

For accuracy analysis of the ANN-PSO-AS designed approach, statistical values are accomplished for 60 executions using minimum (Min), Mean, semi-interquartile range (SI-R) and median (MED) to solve the second order SMP-DD model-based examples (Examples 1–3). SI-R is the $0.5 * (Q_3 - Q_1)$, where Q_1 and Q_3 are the respective first and third quartiles. The Min, Mean, SI-R and MED statistic measures are given in Table 2 to solve the SMP-DD equations. It is indicated that the Min values lie around 10^{-06}–10^{-08}, 10^{-06}–10^{-09} and 10^{-06}–10^{-08} ranges for Examples 1–3. The mean, MED and SI-R values are found in 10^{-04}–10^{-06}

Table 2 Statistics Results for the Second-order SMP-DD Model-based Examples (Examples 1–3).

χ	Example 1				Example 2				Example 3			
	Min	**Mean**	**MED**	**SI-R**	**Min**	**Mean**	**MED**	**SI-R**	**Min**	**Mean**	**MED**	**SI-R**
0	3×10^{-08}	1×10^{-05}	1×10^{-06}	1×10^{-06}	7×10^{-08}	7×10^{-06}	2×10^{-06}	2×10^{-06}	4×10^{-08}	6×10^{-06}	1×10^{-06}	2×10^{-06}
0.05	5×10^{-08}	1×10^{-05}	4×10^{-06}	4×10^{-06}	2×10^{-07}	1×10^{-05}	4×10^{-06}	3×10^{-06}	4×10^{-08}	1×10^{-05}	4×10^{-06}	2×10^{-06}
0.1	1×10^{-07}	2×10^{-05}	6×10^{-06}	5×10^{-06}	1×10^{-07}	1×10^{-05}	7×10^{-06}	5×10^{-06}	1×10^{-07}	1×10^{-05}	5×10^{-06}	4×10^{-06}
0.15	5×10^{-08}	3×10^{-05}	6×10^{-06}	7×10^{-06}	2×10^{-07}	4×10^{-05}	1×10^{-05}	7×10^{-06}	6×10^{-08}	2×10^{-05}	7×10^{-06}	6×10^{-06}
0.2	2×10^{-07}	8×10^{-05}	2×10^{-05}	1×10^{-05}	3×10^{-07}	1×10^{-04}	3×10^{-05}	2×10^{-05}	3×10^{-08}	4×10^{-05}	1×10^{-05}	2×10^{-05}
0.25	1×10^{-06}	1×10^{-04}	3×10^{-05}	3×10^{-05}	1×10^{-06}	2×10^{-04}	5×10^{-05}	4×10^{-05}	2×10^{-06}	8×10^{-05}	4×10^{-05}	3×10^{-05}
0.3	1×10^{-06}	2×10^{-04}	6×10^{-05}	5×10^{-05}	1×10^{-07}	4×10^{-04}	8×10^{-05}	6×10^{-05}	2×10^{-06}	1×10^{-04}	6×10^{-05}	4×10^{-05}
0.35	3×10^{-07}	3×10^{-04}	8×10^{-05}	7×10^{-05}	5×10^{-06}	5×10^{-04}	1×10^{-04}	8×10^{-05}	6×10^{-07}	1×10^{-04}	9×10^{-05}	6×10^{-05}
0.4	1×10^{-07}	3×10^{-04}	9×10^{-05}	8×10^{-05}	6×10^{-06}	6×10^{-04}	1×10^{-04}	1×10^{-04}	3×10^{-06}	1×10^{-04}	1×10^{-04}	7×10^{-05}
0.45	5×10^{-08}	4×10^{-04}	1×10^{-04}	1×10^{-04}	3×10-09	7×10^{-04}	1×10^{-04}	1×10^{-04}	2×10^{-06}	2×10^{-04}	1×10^{-04}	8×10^{-05}
0.5	4×10^{-06}	4×10^{-04}	1×10^{-04}	1×10^{-04}	5×10^{-06}	7×10^{-04}	1×10^{-04}	1×10^{-04}	1×10^{-06}	2×10^{-04}	1×10^{-04}	8×10^{-05}
0.55	3×10^{-06}	5×10^{-04}	1×10^{-04}	1×10^{-04}	1×10^{-06}	7×10^{-04}	2×10^{-04}	1×10^{-04}	4×10^{-07}	2×10^{-04}	1×10^{-04}	8×10^{-05}
0.6	2×10^{-06}	5×10^{-04}	1×10^{-04}	1×10^{-04}	1×10^{-06}	7×10^{-04}	2×10^{-04}	1×10^{-04}	7×10^{-08}	2×10^{-04}	1×10^{-04}	1×10^{-04}
0.65	1×10^{-06}	5×10^{-04}	1×10^{-04}	1×10^{-04}	6×10^{-06}	7×10^{-04}	2×10^{-04}	1×10^{-04}	1×10^{-06}	2×10^{-04}	1×10^{-04}	1×10^{-04}
0.7	1×10^{-07}	4×10^{-04}	1×10^{-04}	1×10^{-04}	6×10^{-06}	6×10^{-04}	2×10^{-04}	1×10^{-04}	7×10^{-07}	2×10^{-04}	1×10^{-04}	9×10^{-05}
0.75	1×10^{-06}	4×10^{-04}	1×10^{-04}	1×10^{-04}	5×10^{-06}	5×10^{-04}	1×10^{-04}	1×10^{-04}	1×10^{-07}	2×10^{-04}	1×10^{-04}	8×10^{-05}
0.8	3×10^{-06}	3×10^{-04}	1×10^{-04}	1×10^{-04}	7×10^{-06}	4×10^{-04}	1×10^{-04}	9×10^{-05}	1×10^{-06}	2×10^{-04}	1×10^{-04}	8×10^{-05}
0.85	2×10^{-06}	3×10^{-04}	9×10^{-05}	9×10^{-05}	1×10^{-06}	3×10^{-04}	1×10^{-04}	7×10^{-05}	3×10^{-08}	2×10^{-04}	1×10^{-04}	8×10^{-05}
0.9	2×10^{-06}	2×10^{-04}	6×10^{-05}	7×10^{-05}	2×10^{-06}	2×10^{-04}	1×10^{-04}	9×10^{-05}	3×10^{-06}	2×10^{-04}	1×10^{-04}	9×10^{-05}
0.95	8×10^{-07}	2×10^{-04}	5×10^{-05}	6×10^{-05}	1×10-10	1×10^{-04}	8×10^{-05}	9×10^{-05}	1×10^{-08}	1×10^{-04}	9×10^{-05}	7×10^{-05}
1	1×10^{-07}	1×10^{-04}	3×10^{-05}	6×10^{-05}	2×10^{-06}	2×10^{-04}	6×10^{-05}	7×10^{-05}	5×10^{-07}	1×10^{-04}	8×10^{-05}	6×10^{-05}

region for all examples. These values stipulate very good measures for the SMP-DD model.

5. CONCLUSION

The design of the numerical computing solver ANN-PSO-AS is presented to solve second-order SMP-DD system and the outcomes are precise, stable and consistent using the ANNs competency of regression. An MF of the networks is designed based on the error function and accordingly optimization with local and global capabilities of the AS approach and PSO, respectively. The ANN-PSO-AS approach is accomplished to solve three different examples of the second-order SMP-DD model. The precise performance of ANN-PSO-AS approach is verified through AE within reasonable accuracy, i.e. around 6–8 decimals of precision from the true/exact outcomes for all variants of the SMP-DD equations. The statistical investigations on Min, SI-R, Mean and MED indices further certified the robustness, stability and precision of ANN-PSO-AS approach for solving the second-order SMP-DDsystem.

In the future, the ANN-PSO-AS algorithm-based accurate stochastic numerical procedure can be implemented for higher order functional differential model,[56,57] computer virus models,[58,59] mathematical model for information security,[60,61] bioinformatics[62,63] and dynamical analysis of computational fluid mechanics problems.[64–66]

REFERENCES

1. L. Bogachev, G. Derfel, S. Molchanov and J. Ochendon, On bounded solutions of the balanced generalized pantograph equation, in *Topics in Stochastic Analysis and Nonparametric Estimation*, The IMA Volumes in Mathematics and its Applications, Vol. 145, eds. P.-L. Chow, G. Yin and B. Mordukhovich (Springer, New York, 2008), pp. 29–49.
2. S. K. Vanani, J. S. Hafshejani, F. Soleymani and M. Khan, On the numerical solution of generalized pantograph equation, *World Appl. Sci. J.* **13**(12) (2011) 2531–2535.
3. M. Z. Liu and D. S. Li, Properties of analytic solution and numerical solution of multi-pantograph equation, *Appl. Math. Comput.* **155** (2004) 853–871.
4. M. Sezer, A method for the approximate solution of the secondorder linear differential equations in terms of Taylor polynomials, *Int. J. Math. Educ. Sci. Technol.* **27**(6) (1996) 821–834.
5. P. Kelevedjiev, Existence of positive solutions to a singular second order boundary value problem, *Nonlinear Anal.* **50** (2002) 1107–1118.
6. Y. S. Liu and H. M. Yu, Existence and uniquess of positive solution for singular boundary value problem, *Comput. Math. Appl.* **50** (2005) 133–143.
7. M. Sezer, S. Yalcinbas and N. Sahin, Approximate solution of multi-pantograph equation with variable coefficients, *Comput. Math.* **7** (2007) 1–11.
8. P. Du and F. Geng, A new method of solving singular multi-pantograph delay differential equation in reproducing kernel space, *Appl. Math. Sci.* **27**(2) (2008) 1299–1305.
9. M. S. Bahgat, Approximate analytical solution of the linear and nonlinear multi-pantograph delay differential equations, *Phys. Script.* **95**(5) (2020) 055219.
10. S. A. Yousefi, M. Noei-Khorshidi and A. Lotfi, Convergence analysis of least squares-Epsilon–Ritz algorithm for solving a general class of pantograph equations, *Kragujevac J. Math.* **42**(3) (2018) 431–439.
11. Y. Yang and E. Tohidi, Numerical solution of multi-Pantograph delay boundary value problems via an efficient approach with the convergence analysis, *Comput. Appl. Math.* **38**(3) (2019) 127.
12. M. A. Z. Raja, J. A. Khan, A. Zameer, N. A. Khan and M. A. Manzar, Numerical treatment of nonlinear singular Flierl–Petviashivili systems using neural networks models, *Neural Comput. Appl.* **31** (2019) 2371–2394.
13. M. A. Z. Raja, S. Abbas, M. I. Syam and A. M. Wazwaz, Design of neuro-evolutionary model for solving nonlinear singularly perturbed boundary value problems, *Appl. Soft Comput.* **62** (2018) 373–394.
14. C. J. Zúñiga-Aguilar, A. Coronel-Escamilla, J. F. Gómez-Aguilar, V. M. Alvarado-Martínez and H. M. Romero-Ugalde, New numerical approximation for solving fractional delay differential equations of variable order using artificial neural networks, *Eur. Phys. J. Plus* **133**(2) (2018) 75.
15. I. Ahmad *et al.*, Neuro-evolutionary computing paradigm for Painlevé equation-II in nonlinear optics, *Eur. Phys. J. Plus* **133**(5) (2018) 184.
16. Z. Sabir *et al.*, Neuro-heuristics for nonlinear singular Thomas–Fermi systems, *Appl. Soft Comput.* **65** (2018) 152–169.
17. A. H. Bukhari, M. A. Z. Raja, M. Sulaiman, S. Islam, M. Shoaib and P. Kumam, Fractional neuro-sequential ARFIMA-LSTM for financial market forecasting, *IEEE Access* **8** (2020) 71326–71338.
18. M. Umar *et al.*, A stochastic computational intelligent solver for numerical treatment of mosquito dispersal model in a heterogeneous environment, *Eur. Phys. J. Plus* **135**(7) (2020) 1–23.

19. Z. Sabir *et al.*, Design of stochastic numerical solver for the solution of singular three-point second-order boundary value problems, *Neural Comput. Appl.* (2020), https://doi.org/10.1007/s00521-020-05143-8.
20. M. Umar *et al.*, Intelligent computing for numerical treatment of nonlinear prey–predator models, *Appl. Soft Comput.* **80** (2019) 506–524.
21. Z. Sabir *et al.*, Heuristic computing technique for numerical solutions of nonlinear fourth order Emden–Fowler equation, *Math. Comput. Simul.* **178** (2020) 534–548.
22. M. A. Z. Raja, F. H. Shah, M. Tariq and I. Ahmad, Design of artificial neural network models optimized with sequential quadratic programming to study the dynamics of nonlinear Troesch's problem arising in plasma physics, *Neural Comput. Appl.* **29**(6) (2018) 83–109.
23. A. Mehmood *et al.*, Design of neuro-computing paradigms for nonlinear nanofluidic systems of MHD Jeffery–Hamel flow, *J. Taiwan Inst. Chem. Eng.* **91** (2018) 57–85.
24. Z. Sabir *et al.*, Novel design of Morlet wavelet neural network for solving second order Lane–Emden equation, *Math. Comput. Simul.* **172** (2020) 1–14.
25. A. Mehmood *et al.*, Intelligent computing to analyze the dynamics of magnetohydrodynamic flow over stretchable rotating disk model, *Appl. Soft Comput.* **67** (2018) 8–28.
26. M. A. Z. Raja, F. H. Shah, E. S. Alaidarous and M. I. Syam, Design of bio-inspired heuristic technique integrated with interior-point algorithm to analyze the dynamics of heartbeat model, *Appl. Soft Comput.* **52** (2017) 605–629.
27. I. Ahmad *et al.*, Integrated neuro-evolution-based computing solver for dynamics of nonlinear corneal shape model numerically, *Neural Comput. Appl.* (2020), https://doi.org/10.1007/s00521-020-05355-y.
28. M. A. Z. Raja, J. Mehmood, Z. Sabir, A. K. Nasab and M. A. Manzar, Numerical solution of doubly singular nonlinear systems using neural networks-based integrated intelligent computing, *Neural Comput. Appl.* **31**(3) (2019) 793–812.
29. A. Mehmood *et al.*, Integrated computational intelligent paradigm for nonlinear electric circuit models using neural networks, genetic algorithms and sequential quadratic programming, *Neural Comput. Appl.*, doi: https://doi.org/10.1007/s00521-019-04573-3.
30. I. Ahmad *et al.*, Novel applications of intelligent computing paradigms for the analysis of nonlinear reactive transport model of the fluid in soft tissues and microvessels. *Neural Comput. Appl.* **31**(12) (2019) 9041–9059.
31. M. Umar, Z. Sabir, M. A. Z. Raja and Y. G. Sánchez, A stochastic numerical computing heuristic of SIR nonlinear model based on dengue fever, *Res. Phys.* **19** (2020) 103585.
32. M. Umar *et al.*, Stochastic numerical technique for solving HIV infection model of CD4+T cells, *Eur. Phys J. Plus* **135**(6) (2020) 403.
33. Z. Sabir *et al.*, Neuro-swarm intelligent computing to solve the second-order singular functional differential model, *Eur. Phys. J. Plus* **135**(6) 474.
34. Z. Sabir, H. A. Wahab, M. Umar and F. Erdoğan, Stochastic numerical approach for solving second order nonlinear singular functional differential equation, *Appl. Math. Comput.* **363** (2019) 124605.
35. M. A. Z. Raja, M. A. Manzar and R. Samar, An efficient computational intelligence approach for solving fractional order Riccati equations using ANN and SQP, *Appl. Math. Model.* **39**(10–11) (2015) 3075–3093.
36. Z. Sabir *et al.*, FMNEICS: Fractional Meyer neuro-evolution-based intelligent computing solver for doubly singular multi-fractional order Lane–Emden system, *Comput. Appl. Math.* **39**(4) (2020) 1–18.
37. I. Jadoon *et al.*, Integrated meta-heuristics finite difference method for the dynamics of nonlinear unipolar electrohydrodynamic pump flow model, *Appl. Soft Comput.* **97** (2020) 106791.
38. T. N. Cheema *et al.*, Intelligent computing with Levenberg–Marquardt artificial neural networks for nonlinear system of COVID-19 epidemic model for future generation disease control, *Eur. Phys. J. Plus* **135**(11) (2020) 1–35.
39. Z. Shah *et al.*, Design of neural network based intelligent computing for numerical treatment of unsteady 3D flow of Eyring–Powell magneto-nanofluidic model, *J. Mater. Res. Technol.* **9**(6) (2020) 14372–14387.
40. A. H. Bukhari *et al.*, Design of a hybrid NAR-RBFs neural network for nonlinear dusty plasma system, *Alexan. Eng. J.* **59**(5) (2020) 3325–3345.
41. M. H. Taheri, M. Abbasi and M. K. Jamei, Application of an artificial neural network to predict the entrance length of three-dimensional magnetohydrodynamics channel flow, *Eur. Phys. J. Plus* **134**(9) (2019) 471.
42. F. Nasirzadehroshenin, M. Sadeghzadeh, A. Khadang, H. Maddah, M. H. Ahmadi, H. Sakhaeinia and L. Chen, Modeling of heat transfer performance of carbon nanotube nanofluid in a tube with fixed wall temperature by using ANN–GA, *Eur. Phys. J. Plus* **135**(2) (2020) 1–20.
43. L. Brezočnik, I. Fister and V. Podgorelec, Swarm intelligence algorithms for feature selection: Areview, *Appl. Sci.* **8**(9) (2018) 1521.
44. O. Zedadra, A. Guerrieri, N. Jouandeau, G. Spezzano, H. Seridi and G. Fortino, Swarm

intelligence-based algorithms within IoT-based systems: A review, *J. Parallel Distrib. Comput.* **122** (2018) 173–187.
45. S. Akbar *et al.*, Novel application of FO-DPSO for 2-D parameter estimation of electromagnetic plane waves, *Neural Comput. Appl.* **31**(8) (2019) 3681–3690.
46. A. Mehmood, A. Zameer, M. S. Aslam and M. A. Z. Raja, Design of nature-inspired heuristic paradigm for systems in nonlinear electrical circuits, *Neural Comput. Appl.* **32**(11) (2020) 7121–7137.
47. A. Duary, M. S. Rahman, A. A. Shaikh, S. T. A. Niaki and A. K. Bhunia, A new hybrid algorithm to solve bound-constrained nonlinear optimization problems, *Neural Comput. Appl.* **32**(16) (2020) 12427–12452.
48. Y. Muhammad *et al.*, Design of fractional swarming strategy for solution of optimal reactive power dispatch, *Neural Comput. Appl.* **32** (2020) 10501–10518, https://doi.org/10.1007/s00521-019-04589-9.
49. M. A. Z. Raja, M. S. Aslam, N. I. Chaudhary, M. Nawaz and S. M. Shah, Design of hybrid nature-inspired heuristics with application to active noise control systems, *Neural Comput. Appl.* **31**(7) (2019) 2563–2591.
50. A. Zameer *et al.*, Fractional-order particle swarm based multi-objective PWR core loading pattern optimization, *Ann. Nucl. Energy* **135** (2020) 106982.
51. D. Fan, G. P. Jiang, Y. R. Song, Y. W. Li and G. Chen, Novel epidemic models on PSO-based networks, *J. Theor. Biol.* **477** (2019) 36–43.
52. S. Koehler, C. Danielson and F. Borrelli, A primal-dual active-set method for distributed model predictive control, *Optim. Control Appl. Methods* **38**(3) 399–419.
53. X. Wang and P. M. Pardalos, A modified active set algorithm for transportation discrete network design bi-level problem, *J. Global Optim.* **67**(1–2) (2017) 32–342.
54. C. Shen, L. H. Zhang and W. H. Yang, A filter active-set algorithm for ball/sphere constrained optimization problem. *SIAM J. Optim.* **26**(3) (2016) 1429–1464.
55. M. Azizi, M. Amirfakhrian and M. A. F. Araghi, A fuzzy system based active set algorithm for the numerical solution of the optimal control problem governed by partial differential equation, *Eur. J. Control* **54** (2020) 99–110.
56. I. Khan *et al.*, Design of neural network with Levenberg–Marquardt and Bayesian regularization backpropagation for solving pantograph delay differential equations, *IEEE Access* **8** (2020) 137918–137933.
57. M. A. Z. Raja, I. Ahmad, I. Khan, M. I. Syam and A. M. Wazwaz, Neuro-heuristic computational intelligence for solving nonlinear pantograph systems, *Front. Inform. Technol. Electron. Eng.* **18**(4) (2017) 464–484.
58. Z. Masood *et al.*, Design of epidemic computer virus model with effect of quarantine in the presence of immunity, *Fund. Inform.* **161**(3) (2018) 249–273.
59. A. Raza, M. S. Arif, M. Rafiq, M. Bibi, M. Naveed, M. U. Iqbal, Z. Butt, H. A. Naseem and J. N. Abbasi, Numerical treatment for stochastic computer virus model, *Comput. Model. Eng. Sci.* **120**(2) (2019) 445–465.
60. Z. Masood *et al.*, Design of a mathematical model for the Stuxnet virus in a network of critical control infrastructure, *Comput. Secur.* **87** (2019) 101565.
61. Z. Masood *et al.*, Design of fractional order epidemic model for future generation tiny hardware implants, *Fut. Gen. Comput. Syst.* **106** (2020) 43–54.
62. M. Umar *et al.*, A stochastic intelligent computing with neuro-evolution heuristics for nonlinear SITR system of novel COVID-19 dynamics, *Symmetry* **12**(10) (2020) 1628.
63. M. A. Z. Raja, M. Umar, Z. Sabir, J. A. Khan and D. Baleanu, A new stochastic computing paradigm for the dynamics of nonlinear singular heat conduction model of the human head, *Eur. Phys. J. Plus* **133**(9) (2018) 364.
64. M. Umar *et al.*, Three-dimensional flow of Casson nanofluid over a stretched sheet with chemical reactions, velocity slip, thermal radiation and Brownian motion, *Therm. Sci.* 339–339.
65. Z. Sabir, R. Akhtar, Z. Zhiyu, M. Umar, A. Imran, H. A. Wahab, M. Shoaib and M. A. Z. Raja, A computational analysis of two-phase Casson nanofluid passing a stretching sheet using chemical reactions and gyrotactic microorganisms, *Math. Probl. Eng.* **2019** (2019) 1490571, https://doi.org/10.1155/2019/1490571
66. A. Imran *et al.*, Analysis of MHD and heat transfer effects with variable viscosity through ductus efferentes, *AIP Adv.* **9**(8) (2019) 085320